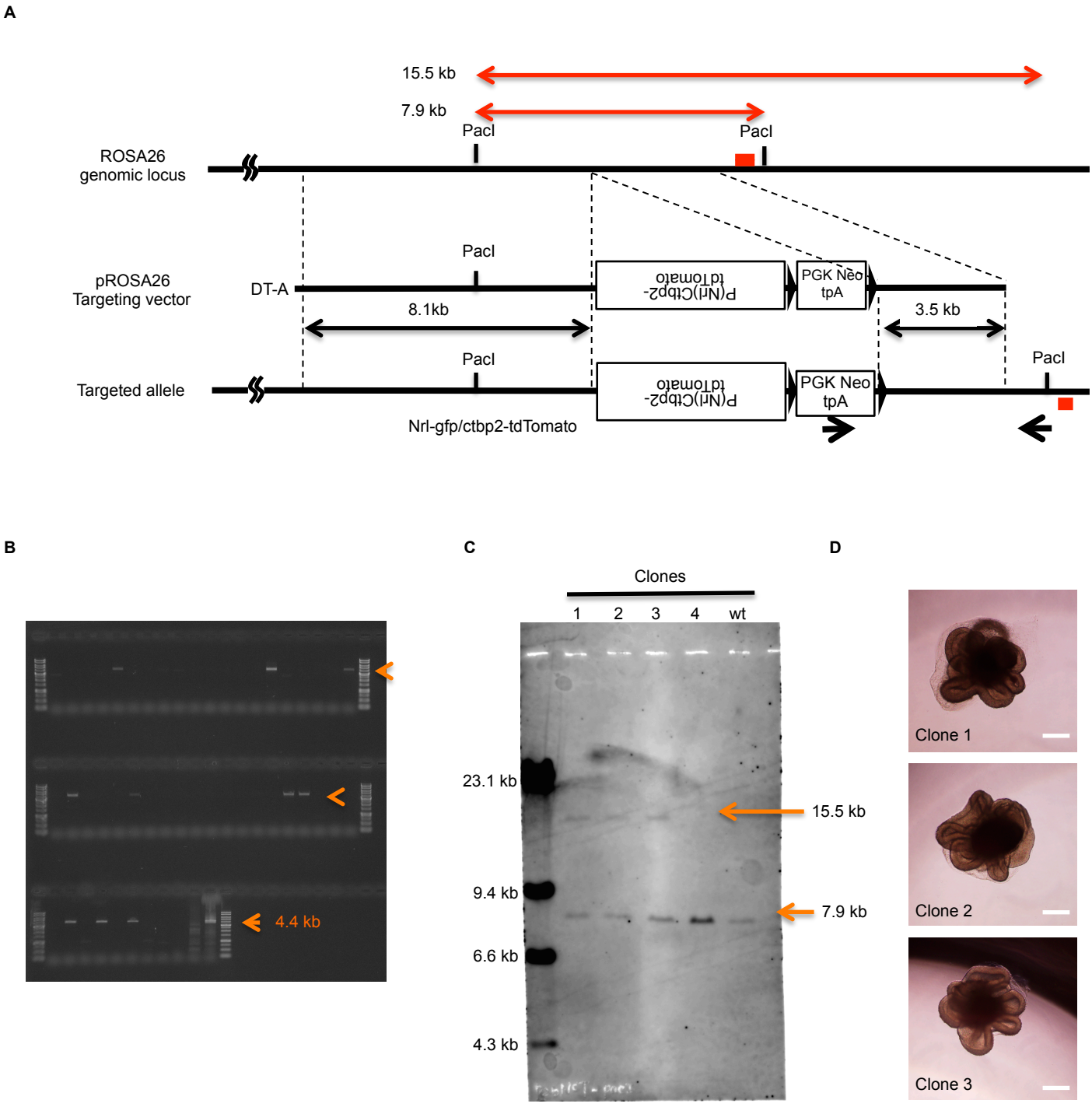

M. Mandai *et al.*, Supplementary Fig.1

Figure S1. Production of CtBP2-labelled cell lines and retinal differentiation (related to Figure 1).

(**A**) Strategy for generating Nrl-GFP/ROSA::CtBP2-tdTomato lines. CtBP2-tdTomato under the mouse *Nrl* promoter was knocked into the ROSA locus in the reverse direction. Black arrows indicate the location of the screening primer pair. Locations of restriction sites by *PacI* and the probe (red bars) for Southern blotting are also shown along with the estimated length of digested products.

(**B**) Screening for homologous recombination.

(**C**) Four positive clones from **B** were confirmed by Southern blotting, and three clones were used for further differentiation.

(**D**) Three clones differentiated into optic vesicle (DD13) structures similarly. Scale bar = 200 μm.

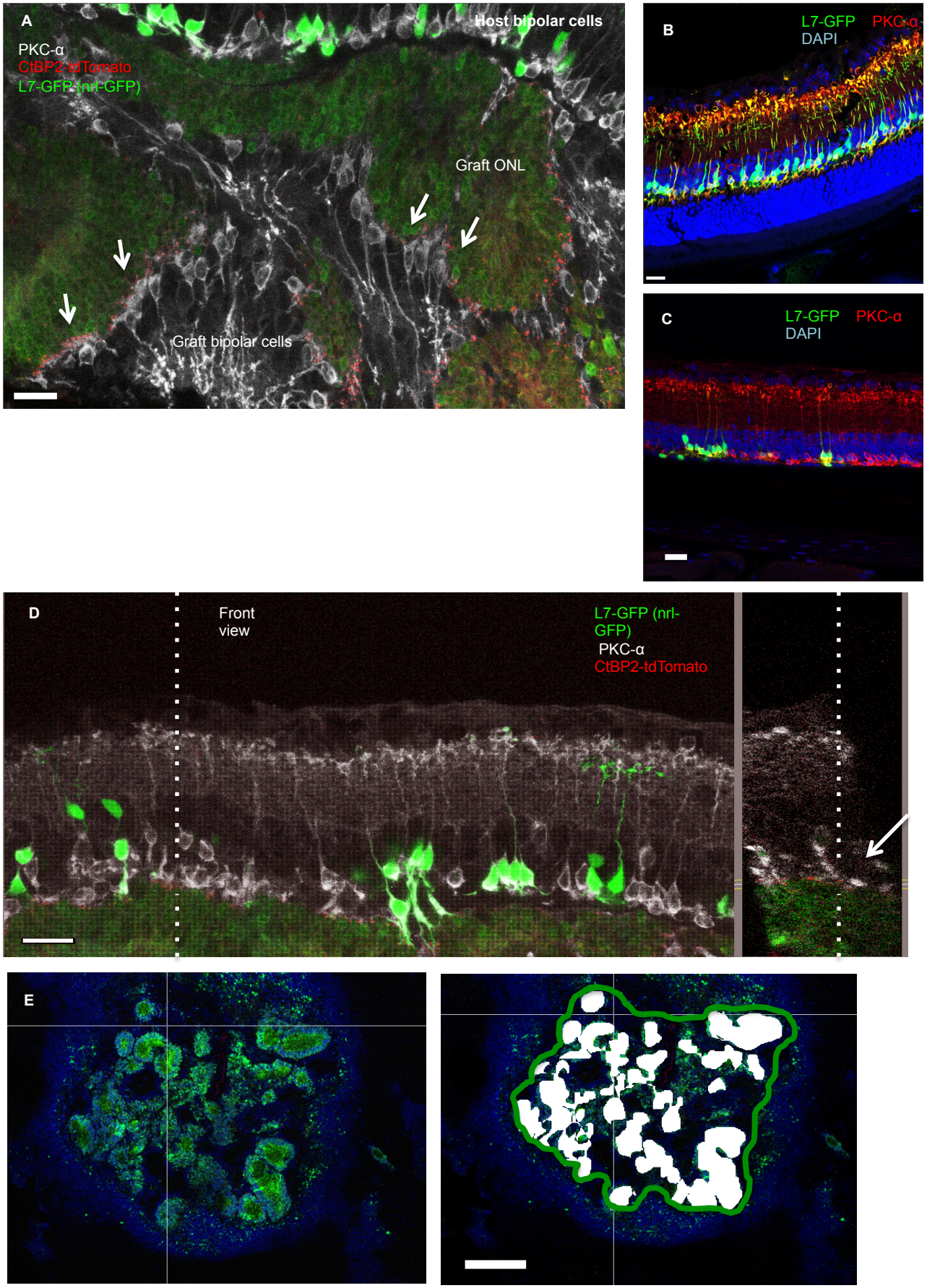

M. Mandai *et al.*, Supplementary Fig.2

Figure S2. L7-GFP expression in *rd* mice, and host-graft contact with and without GFP (related to Figure 2).

(A) Dense CtBP2-tdTomato expression was observed at the dendrite tips of graft bipolar cells at the intra-graft synaptic sites (arrows) on the margin of outer nuclear layer (ONL).

(B, C) L7-GFP expression was reduced in some parts of the *rd1* retina. In the wild-type retina, L7- GFP colocalized with PKC-α immunoreactivity (**B**), whereas in the 12-week-old *rd1* retina, GFP expression was reduced or undetectable in the PKC-α-positive rod bipolar cells in some part of the retina (**C**).

(D) Some GFP-negative PKC-α positive bipolar cells also contacted graft CtBP2 directly (arrow). Front and side views in the plane indicated by each white dotted line.

(E) The area of ONL rosettes (Nrl-GFP positive) that can contact host INL (L7-GFP retina) was estimated as shown in the figure and calculated as a proportion to the total graft area. (50.8 ± 7.8 % , n = 5).; scale bars = 20 μm (**A-D**) and 200 μm (**E**).

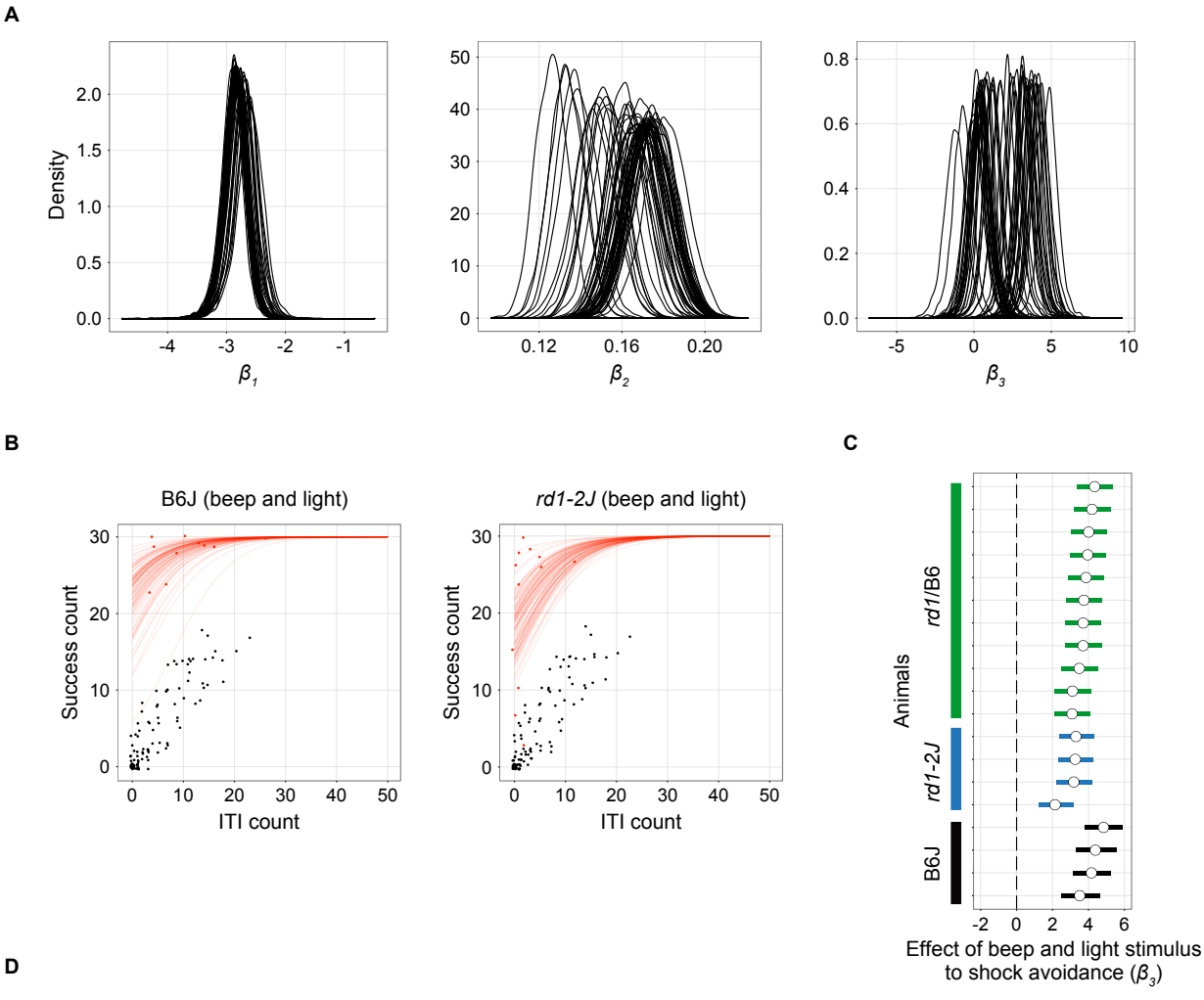

M. Mandai *et al.*, Supplementary Fig. 3

Figure S3. Additional SAS data and an OCT image of successful transplantation (related to Figure 3).

(**A**) Distribution of the estimated parameters of all mice tested by SAS in this study**.** The distributions of β_1, which is the base value of the model, were nearly identical. The distributions of β_2, which is the coefficient of the ITI count, were positive, which is reasonable. The distributions of β_3, which is the coefficient for transplantation, were widely distributed over zero. This result implies that the interference of transplantation has both positive and negative effects on visual function. See Methods for further information.

(**B**) Representative results of the SAS test using simultaneous light and audio (beep) stimulation, for a wild-type B6 (left) and *rd1-2J* (right) mice. Note that mice in both groups avoided shock when the signal included both beep and light. Dots denote the observed SAS results and the lines are estimated relationships of ITI count and SAS success rate simulated from randomly selected posterior samples of the model; black and red indicate the control and the subject, respectively

(**C**) The posterior distributions of the estimated effect of beep & light input to shock avoidance (β_3) of all of the mice that underwent SAS testing.

(**D**) Representative OCT image showing successful transplantation. The number of ONL rosettes was identified by OCT, with the high-intensity area corresponding to inner- or outer-segment-like structures (some of the large rosettes are marked by asterisks). Some of the rosettes may be in contact with the host INL. Mice with successful transplantation were used for SAS analysis.

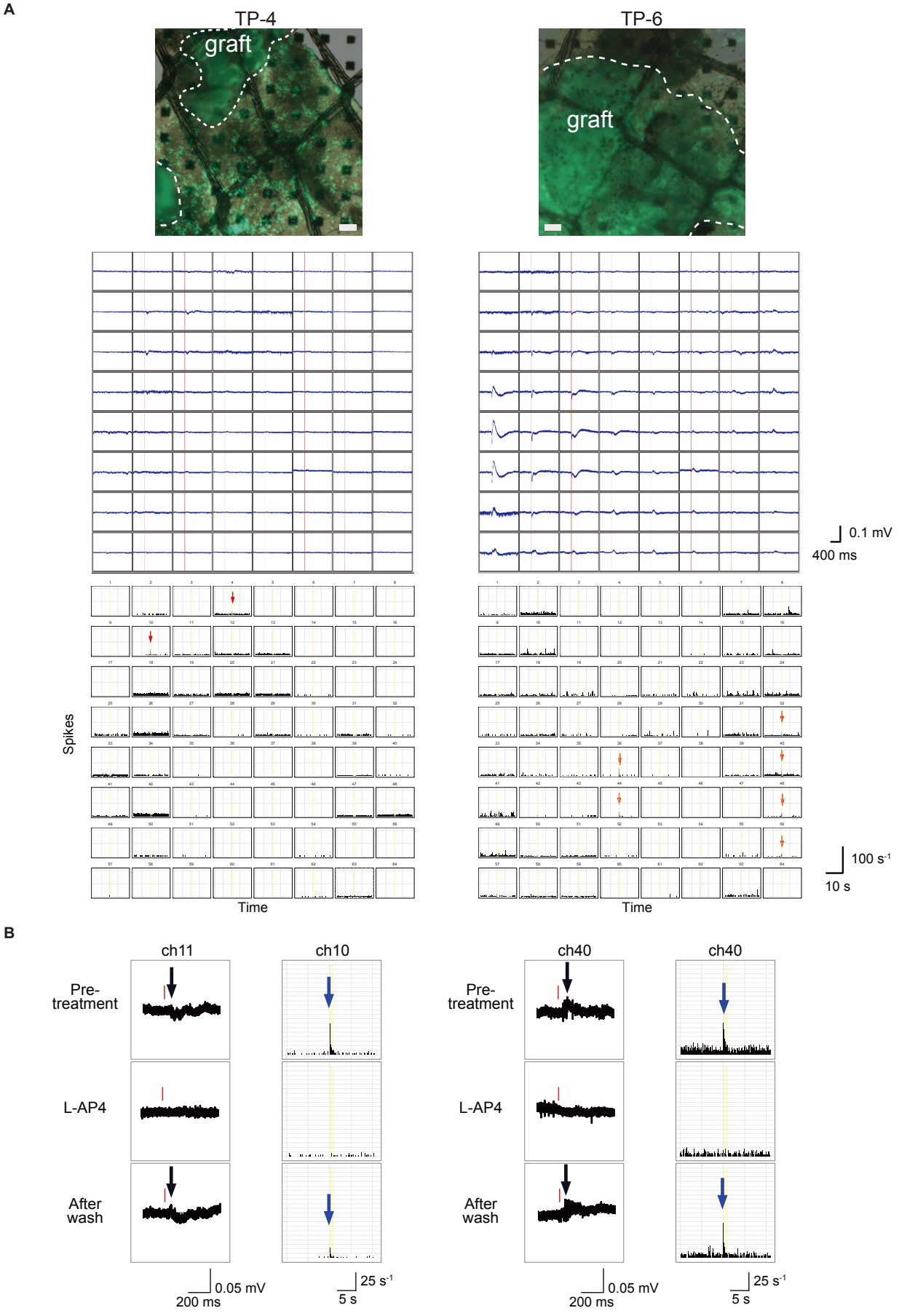

M. Mandai *et al.*, Supplementary Fig. 4

Figure S4. mERG and RGC responses in typical samples (related to Figure 4 and Table 1).

(**A**) The photo images on the MEA electrodes of TP-4 and TP-6 in Table 1 and their responses in mERG and RGC responses after L-AP4 washout (TP-4) and before L-AP4 treatment (TP-6) are presented. Total RGC responses on each channel are shown in histograms after spike sorting. Yellow bands indicate the timing and duration of light signals. Graft area is marked with white dashed lines. The channel presenting typical transient ON responses are marked with red arrows. Scale bars = 100 μm.

(**B**) Recordings of before and after LAP-4 treatment and after washout of channels 10 (RGC recording) and 11 (mERG) for TP-4 and the channel 40 for TP-6 are shown.

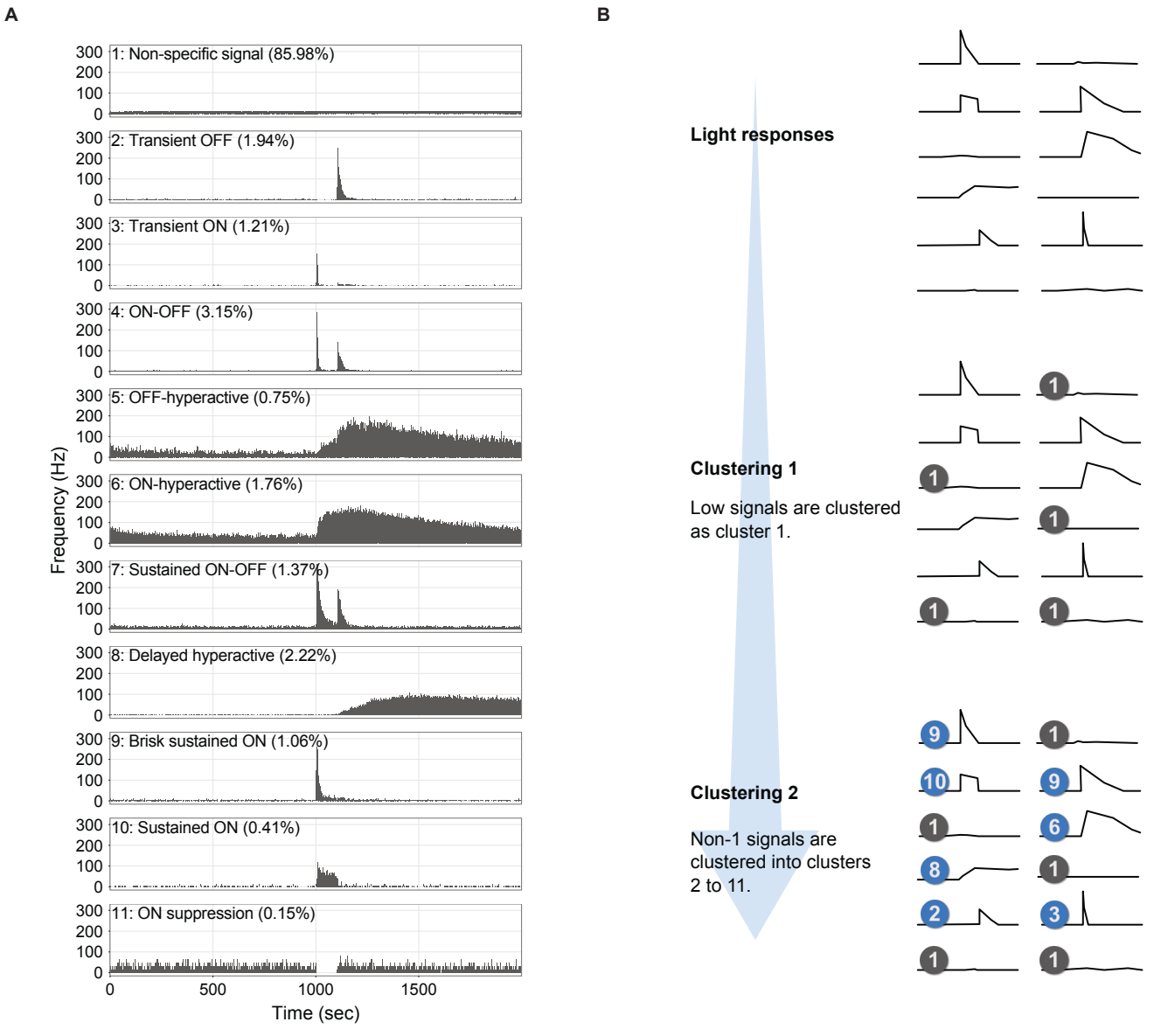

M. Mandai *et al.*, Supplementary Fig. 5

Figure S5. Classification of light responses by deep learning (related to Figure 5).

(**A**) The training dataset was manually clustered into 11 clusters: non-specific response, transient OFF, transient ON, ON-OFF, OFF-hyperactive, ON hyperactive, sustained ON-OFF, delayed hyperactive, brisk sustained ON, sustained ON, and ON suppression, based on the pattern of responses to the light stimuli.

(**B**) Flowchart of light-response clustering. First, the light responses recorded by MEA were spike-sorted. Individualized light responses were then clustered by a deep-learning model (model 1) to distinguish between cluster 1s and non-1s. Finally, the non-1 responses were clustered by another deep-learning model (model 2) into clusters 2 to 11.